

# 1-Aryl-3,5-dimethylpyrazolium based tunable protic ionic liquids (TPILs)

Melek Canbulat Özdemir <sup>a,\*</sup>, Beytiye Özgün <sup>b</sup>, Ebru Aktan <sup>b</sup>

<sup>a</sup> Department of Environmental Engineering, Faculty of Engineering, Middle East Technical University, 06800, Ankara, Turkey

<sup>b</sup> Department of Chemistry, Faculty of Science, Gazi University, 06500 Teknikokullar, Ankara, Turkey

## ARTICLE INFO

### Article history:

Received 1 June 2018

Received in revised form

27 November 2018

Accepted 6 December 2018

Available online 7 December 2018

### Keywords:

Pyrazolium cations [Ph<sub>R</sub>Hpz]<sup>+</sup>

Tunable protic ionic liquids (TPILs)

Substituent effects

DFT

## ABSTRACT

A series of new 1-aryl-3,5-dimethylpyrazolium based tunable protic ionic liquids/salts ([Ph<sub>R</sub>Hpz][X], R: –H, –Cl, –Br, –CH<sub>3</sub>, –OCH<sub>3</sub>, X: chloride [Cl<sup>–</sup>] and tetrafluoroborate [BF<sub>4</sub><sup>–</sup>]) have been synthesized through acid-base neutralization reactions between 1-aryl-3,5-dimethyl-1H-pyrazoles and the corresponding inorganic acids. The chemical structure of the salts was confirmed by FTIR, <sup>1</sup>H NMR, <sup>13</sup>C NMR, elemental analysis, and <sup>19</sup>F NMR (3a–3e) and the crystal structure of the two salts (2a and 3d) was also elucidated by X-ray analysis of single crystals. Melting points and thermal decomposition temperatures of TPILs (2e and 3b) were determined. The geometries of the cations, anions and ionic salts were optimized, and their molecular electrostatic potentials (MEPs) were assessed by using density functional theory methods (B3LYP and M06-2X). The electrochemical window of the salts was determined both experimentally and theoretically. The correlation coefficient values were also calculated by using theoretical and experimental EW values of the salts.

© 2018 Elsevier B.V. All rights reserved.

## 1. Introduction

Protic ionic liquids (PILs) are a subclass of ionic liquids (ILs) which are easily prepared through the proton transfer from a Bronsted acid to a Bronsted base [1,2]. Compared to aprotic ionic liquids (AILs), which generally require more complex synthesis and purification procedures, the synthesis of PILs is simple as both the preparation and purification processes [3–5]. Another distinctive feature of PILs is their capacity to build up hydrogen-bonded networks. The proton transfer from the acid to the base constitutes proton donor and acceptor sites and can lead to the generation of hydrogen bonds [6–9]. Owing to their special properties PILs have been utilized in a variety of applications such as electrochemistry [10–12], catalysis and organic synthesis [13–18], and biological applications [19], etc.

The physical and chemical properties of ILs are mainly controlled by intermolecular forces and are easily tuned by a possible combination of the cations and anions. To date, numerous studies have been conducted to the study of the effects of cation structure on the physicochemical properties of ILs [20–24]. In our previous works, we have synthesized 3,5-dimethylpyrazolium

based tunable aryl alkyl ionic liquids (TAAILs) and investigated the effects of para substituent and alkyl chain length on the properties of synthesized salts [25,26]. Unlike the known dialkylsubstituted ILs, TAAILs have additional possibilities to tune the system through additional steric and electronic effects.

To the best of our knowledge, 1-aryl-3,5-dimethylpyrazole based protic ionic liquids have not been explored before. In the present work, new protic 1-aryl-3,5-dimethylpyrazolium based ionic liquids/salts which have [Cl<sup>–</sup>] and [BF<sub>4</sub><sup>–</sup>] anions were synthesized and characterized. The influence of both the electron withdrawing and the electron donating substituents (–Cl, –Br, –H, –Me, –OMe) at the para position of the phenyl ring on the thermal properties of the salts has been investigated. The geometries of the synthesized salts were optimized, and their molecular electrostatic potentials (MEPs) were assessed by using density functional theory methods (B3LYP and M06-2X). The EW of the salts was determined both experimentally and theoretically and the correlation coefficient values were calculated.

## 2. Experimental section

### 2.1. Materials and instrumentation

All solvents and reagents were obtained commercially and used without further purification. Multimode oven (Microsynth -

\* Corresponding author.

E-mail address: [ozmelek@metu.edu.tr](mailto:ozmelek@metu.edu.tr) (M.C. Özdemir).

Milestone) were used for microwave-assisted reactions. FTIR spectra were obtained from samples with an ATR (Attenuated Total Reflectance) accessory. NMR spectra were recorded on a Bruker-Avance-300 MHz spectrometer (at 300 MHz for  $^1\text{H}$  NMR, 75 MHz for  $^{13}\text{C}$  NMR and 282 MHz for  $^{19}\text{F}$  NMR) with TMS as an internal standard in  $\text{CDCl}_3$  or  $\text{DMSO}-d_6$ . Elemental analysis was carried out using a LECO, CHNS-932 elemental analyzer. All melting points were determined with Electrothermal 9200 melting point apparatus. The thermal stability of the ionic liquids (2e and 3b) was investigated on a SII Extra TG/DTA 7200 at a heating rate  $10^\circ\text{C min}^{-1}$  with nitrogen as the purge gas.

Cyclic Voltammetry experiments were conducted with Electrochemical Workstation CHI-660B instrument at  $25^\circ\text{C}$ . Glassy carbon macro electrode (surface area:  $7.065 \times 10^{-2} \text{ cm}^2$ ) was used as a working electrode. Pt and Ag/AgCl electrodes were used as a counter and reference electrode, respectively. The solutions of the synthesized 1-aryl-3,5-dimethylpyrazolium based protic ionic salts (2a–2e and 3a–3e) with a concentration of 0.1 M were prepared in anhydrous acetonitrile. Each solution was purged with nitrogen for at least 10 min to reduce the effect of water and oxygen on cyclic voltammograms.

## 2.2. Synthesis and characterization

### 2.2.1. Synthesis of 1-aryl-3,5-dimethyl-1H-pyrazole compounds

1-aryl-3,5-dimethyl-1H-pyrazole derivatives were synthesized by a procedure reported in our previous work [26]. In brief, to a solution of arylhydrazinium hydrochloride (5.0 mmol) in acetic acid (30 mL), acetylacetone (5.0 mmol) was added with continuous stirring. The solution was heated at  $120^\circ\text{C}$  under MW irradiation until all the starting materials were consumed (TLC, 20% EtOAc–hexane). After completion of the reaction, the solvent was removed under reduced pressure, and the residue was dissolved in ethyl acetate. The organic layer was washed with diluted sodium hydrogen carbonate, water, and saturated brine, respectively and dried over anhydrous sodium sulfate. Then, the solvent was evaporated, and the crude product was purified with silica gel column chromatography.

3,5-dimethyl-1-phenyl-1H-pyrazole (1a): Irradiation time: 2.0 min. Yield: 90% (orange oil);  $^1\text{H}$  NMR (300 MHz,  $\text{DMSO}-d_6$ , ppm):  $\delta = 2.18$  (s, 3H,  $\text{CH}_3$ ); 2.28 (s, 3H,  $\text{CH}_3$ ); 6.05 (s, 1H, CH); 7.35–7.48 (m, 5H, Ph).  $^{13}\text{C}$  NMR (75 MHz,  $\text{DMSO}-d_6$ , ppm):  $\delta = 12.57$ ; 13.72; 107.55; 124.47; 127.32; 129.45; 139.48; 140.16; 148.26.

1-(*p*-chlorophenyl)-3,5-dimethyl-1H-pyrazole (1b): Irradiation time: 1.5 min. Yield: 95% (orange oil);  $^1\text{H}$  NMR (300 MHz,  $\text{CDCl}_3$ , ppm):  $\delta = 2.29$  (s, 3H,  $\text{CH}_3$ ); 2.30 (s, 3H,  $\text{CH}_3$ ); 6.0 (s, 1H, CH); 7.36–7.43 (m, 4H, Ph).  $^{13}\text{C}$  NMR (75 MHz,  $\text{CDCl}_3$ , ppm):  $\delta = 12.24$ ; 13.36; 107.41; 125.43; 128.94; 132.47; 138.43; 139.15; 149.05.

1-(*p*-bromophenyl)-3,5-dimethyl-1H-pyrazole (1c): Irradiation time: 2.0 min. Yield: 78% (light brown oil);  $^1\text{H}$  NMR (300 MHz,  $\text{CDCl}_3$ , ppm):  $\delta = 2.29$  (s, 3H,  $\text{CH}_3$ ); 2.30 (s, 3H,  $\text{CH}_3$ ); 6.0 (s, 1H, CH); 7.31–7.34 (d, 2H, Ph, J: 8.8 Hz); 7.55–7.58 (d, 2H, Ph, J: 8.8 Hz).  $^{13}\text{C}$  NMR (75 MHz,  $\text{CDCl}_3$ , ppm):  $\delta = 12.38$ ; 13.46; 107.51; 120.43; 125.73; 131.95; 138.93; 139.13; 149.12.

1-(*p*-methylphenyl)-3,5-dimethyl-1H-pyrazole (1d): Irradiation time: 1.5 min. Yield: 90% (orange oil);  $^1\text{H}$  NMR (300 MHz,  $\text{CDCl}_3$ , ppm):  $\delta = 2.28$  (s, 3H,  $\text{CH}_3$ ); 2.30 (s, 3H,  $\text{CH}_3$ ); 2.40 (s, 3H,  $\text{CH}_3$ ); 5.98 (s, 1H, CH); 7.23–7.25 (d, 2H, Ph, J: 8.4 Hz); 7.29–7.32 (d, 2H, Ph, J: 8.4 Hz).  $^{13}\text{C}$  NMR (75 MHz,  $\text{CDCl}_3$ , ppm):  $\delta = 12.27$ ; 13.51; 21.04; 106.60; 124.66; 129.51; 137.07; 137.49; 139.30; 148.63.

3,5-dimethyl-1-(*p*-methoxyphenyl)-1H-pyrazole (1e): Irradiation time: 1.0 min. Yield: 90% (brown oil);  $^1\text{H}$  NMR (300 MHz,

$\text{CDCl}_3$ , ppm):  $\delta = 2.25$  (s, 3H,  $\text{CH}_3$ ); 2.29 (s, 3H,  $\text{CH}_3$ ); 3.84 (s, 3H,  $\text{CH}_3$ ); 6.0 (s, 1H, CH); 6.94–6.97 (d, 2H, Ph, J: 8.9 Hz); 7.31–7.34 (d, 2H, Ph, J: 8.9 Hz).  $^{13}\text{C}$  NMR (75 MHz,  $\text{CDCl}_3$ , ppm):  $\delta = 12.12$ ; 13.49; 55.49; 106.24; 114.09; 126.34; 133.10; 139.44; 148.48; 158.76.

### 2.2.2. General procedure for the synthesis of 1-aryl-3,5-dimethylpyrazolium salts

Protic pyrazolium salts were readily prepared according to a Brønsted acid-base reaction carried out in a stoichiometric ratio. To a stirred solution of 1-aryl-3,5-dimethyl-1H-pyrazole compound (5 mmol) in a small amount of ethanol (5 mL) at room temperature, was carefully added concentrated hydrochloric acid (5 mmol, 37%) for compounds 2a–2e, and tetrafluoroboric acid (5 mmol, 48% in water) for compounds 3a–3e. The reaction mixture was cooled to room temperature and stirred for 30 min at room temperature. After evaporation of solvent the product was washed with hexane (10 mL) and diethyl ether (10 mL), respectively. The crude product was dissolved in acetonitrile (10 mL), active charcoal was added and the mixture was heated under reflux conditions for 2 h. After filtration, the solvent was removed under reduced pressure. Subsequently, the synthesized salts were recrystallized in ethanol and dried in vacuum at  $75^\circ\text{C}$  for 48 h.

3,5-dimethyl-1-phenylpyrazolium chloride (2a): Yield: 89% (off white solid); m.p:  $163^\circ\text{C}$ ; IR (ATR,  $\text{cm}^{-1}$ )  $\nu_{\text{max}} = 3254$ ; 3060; 2920–2792; 1678; 1588; 1497; 755; 693.  $^1\text{H}$  NMR (300 MHz,  $\text{CDCl}_3$ , ppm):  $\delta = 2.37$  (s, 3H, 5- $\text{CH}_3$ ); 2.62 (s, 3H, 3- $\text{CH}_3$ ); 6.36 (s, 1H, CH); 7.57 (m, 5H, Ph), 14.5 (brs, 1H, NH).  $^{13}\text{C}$  NMR (75 MHz,  $\text{CDCl}_3$ , ppm):  $\delta = 11.36$ ; 12.01; 108.24; 125.96; 130.03; 130.99; 132.95; 144.63; 146.82. Analysis: calcd for  $\text{C}_{11}\text{H}_{13}\text{ClN}_2$ : C 63.31 H 6.28 N 13.42. Found: C 62.77 H 6.32 N 13.31.

1-(*p*-chlorophenyl)-3,5-dimethylpyrazolium chloride (2b): Yield: 90% (milky brown solid); m.p:  $139^\circ\text{C}$ ; IR (ATR,  $\text{cm}^{-1}$ )  $\nu_{\text{max}} = 3440$ ; 3107; 2984–2808; 1673; 1571; 1493; 864; 772.  $^1\text{H}$  NMR (300 MHz,  $\text{CDCl}_3$ , ppm):  $\delta = 2.37$  (s, 3H, 5- $\text{CH}_3$ ); 2.61 (s, 3H, 3- $\text{CH}_3$ ); 6.32 (s, 1H, CH); 7.52 (m, 4H, Ph), 13.3 (brs, 1H, NH).  $^{13}\text{C}$  NMR (75 MHz,  $\text{CDCl}_3$ , ppm):  $\delta = 11.48$ ; 11.96; 108.29; 127.40; 130.33; 131.51; 137.23; 144.52; 147.31. Analysis: calcd for  $\text{C}_{11}\text{H}_{12}\text{Cl}_2\text{N}_2$ : C 54.34 H 4.97 N 11.52. Found: C 53.94 H 5.02 N 11.44.

1-(*p*-bromophenyl)-3,5-dimethylpyrazolium chloride (2c): Yield: 92% (milky brown solid); m.p:  $142^\circ\text{C}$ ; IR (ATR,  $\text{cm}^{-1}$ )  $\nu_{\text{max}} = 3268$ ; 3078; 2972–2783; 1703; 1589; 1486; 836; 771.  $^1\text{H}$  NMR (300 MHz,  $\text{CDCl}_3$ , ppm):  $\delta = 2.35$  (s, 3H, 5- $\text{CH}_3$ ); 2.59 (s, 3H, 3- $\text{CH}_3$ ); 6.30 (s, 1H, CH); 7.41–7.44 (d, 2H, Ph, J = 8.70); 7.68–7.71 (d, 2H, Ph, J = 8.70), 13.9 (brs, 1H, NH).  $^{13}\text{C}$  NMR (75 MHz,  $\text{CDCl}_3$ , ppm):  $\delta = 11.44$ ; 11.95; 108.30; 125.36; 127.51; 132.0; 133.29; 144.46; 147.28. Analysis: calcd for  $\text{C}_{11}\text{H}_{12}\text{BrClN}_2$ : C 45.95 H 4.21 N 9.74. Found: C 45.66 H 4.25 N 9.68.

1-(*p*-methylphenyl)-3,5-dimethylpyrazolium chloride (2d): Yield: 93% (milky brown solid); m.p:  $167^\circ\text{C}$ ; IR (ATR,  $\text{cm}^{-1}$ )  $\nu_{\text{max}} = 3426$ ; 3029; 2925–2853; 1642; 1575; 1429; 830; 750.  $^1\text{H}$  NMR (300 MHz,  $\text{CDCl}_3$ , ppm):  $\delta = 2.33$  (s, 3H, 5- $\text{CH}_3$ ); 2.42 (s, 3H, 3- $\text{CH}_3$ ); 2.61 (s, 3H, *p*-( $\text{CH}_3$ )–Ph); 6.27 (s, 1H, CH); 7.37 (m, 4H, Ph).  $^{13}\text{C}$  NMR (75 MHz,  $\text{CDCl}_3$ , ppm):  $\delta = 11.36$ ; 11.84; 21.33; 107.81; 125.80; 130.43; 130.63; 141.60; 144.26; 146.54. Analysis: calcd for  $\text{C}_{12}\text{H}_{15}\text{ClN}_2$ : C 64.71 H 6.79 N 12.58. Found: C 64.2 H 6.82 N 12.48.

3,5-dimethyl-1-(*p*-methoxyphenyl)pyrazolium chloride (2e): Yield: 95% (light-brown solid); m.p:  $62^\circ\text{C}$ ; IR (ATR,  $\text{cm}^{-1}$ )  $\nu_{\text{max}} = 3392$ ; 3065, 2972–2846; 1601; 1514; 1263; 838; 750.  $^1\text{H}$  NMR (300 MHz,  $\text{CDCl}_3$ , ppm):  $\delta = 2.32$  (s, 3H, 5- $\text{CH}_3$ ); 2.59 (s, 3H, 3- $\text{CH}_3$ ); 3.87 (s, 3H, *p*-( $\text{OCH}_3$ )–Ph); 6.24 (s, 1H, CH); 7.03–7.05 (d, 2H, Ph); 7.42–7.44 (d, 2H, Ph).  $^{13}\text{C}$  NMR (75 MHz,  $\text{CDCl}_3$ , ppm):  $\delta = 11.63$ ; 11.92; 55.70; 107.56; 115.07; 126.22; 127.54; 144.0; 146.53; 161.05. Analysis: calcd for  $\text{C}_{12}\text{H}_{15}\text{ClN}_2\text{O}$ : C 60.38 H 6.33 N

11.74. Found: C 59.93 H 6.37 N 11.65.

3,5-dimethyl-1-phenylpyrazolium tetrafluoroborate (3a): Yield: 95% (off-white solid); m.p: 132 °C; IR (ATR,  $\text{cm}^{-1}$ )  $\nu_{\text{max}} = 3221$ ; 3073; 2888–2607; 1596; 1501; 1463; 1437; 1082; 975; 762.  $^1\text{H}$  NMR (300 MHz,  $\text{CDCl}_3$ , ppm):  $\delta = 2.39$  (s, 3H, 5- $\text{CH}_3$ ); 2.56 (s, 3H, 3- $\text{CH}_3$ ); 6.45 (s, 1H, CH); 7.49 (m, 2H, Ph); 7.63 (m, 3H, Ph).  $^{13}\text{C}$  NMR (75 MHz,  $\text{CDCl}_3$ , ppm):  $\delta = 10.92$ ; 11.75; 109.14; 125.66; 130.41; 131.70; 132.49; 147.08; 147.43.  $^{19}\text{F}$  NMR (282 MHz,  $\text{CDCl}_3$ , ppm):  $\delta = -149.58$ ;  $-149.63$ . Analysis: calcd for  $\text{C}_{11}\text{H}_{13}\text{BF}_4\text{N}$ : C 50.81 H 5.04 N 10.77. Found: C 50.46 H 5.08 N 10.7.

1-(p-chlorophenyl)-3,5-dimethylpyrazolium tetrafluoroborate (3b): Yield: 91% (white solid); m.p: 85 °C; IR (ATR,  $\text{cm}^{-1}$ )  $\nu_{\text{max}} = 3418$ ; 3107; 2985–2749; 1587; 1574; 1496; 1432; 1091; 1042; 836.  $^1\text{H}$  NMR (300 MHz,  $\text{CDCl}_3$ , ppm):  $\delta = 2.37$  (s, 3H, 5- $\text{CH}_3$ ); 2.54 (s, 3H, 3- $\text{CH}_3$ ); 6.43 (s, 1H, CH); 7.46–7.49 (d, 2H, Ph,  $J = 8.72$  Hz); 7.58–7.61 (d, 2H, Ph,  $J = 8.72$  Hz).  $^{13}\text{C}$  NMR (75 MHz,  $\text{CDCl}_3$ , ppm):  $\delta = 10.98$ ; 11.70; 109.01; 127.51; 130.64; 131.03; 137.88; 146.85; 147.82.  $^{19}\text{F}$  NMR (282 MHz,  $\text{CDCl}_3$ , ppm):  $\delta = -149.75$ ;  $-149.81$ . Analysis: calcd for  $\text{C}_{11}\text{H}_{12}\text{BClF}_4\text{N}_2$ : C 44.86 H 4.11 N 9.51. Found: C 44.59 H 4.15 N 9.45.

1-(p-bromophenyl)-3,5-dimethylpyrazolium tetrafluoroborate (3c): Yield: 94.5% (off-white solid); m.p: 138 °C; IR (ATR,  $\text{cm}^{-1}$ )  $\nu_{\text{max}} = 3269$ ; 3079; 2930–2785; 1596; 1489; 1437; 1066; 1036; 836.  $^1\text{H}$  NMR (300 MHz,  $\text{CDCl}_3$ , ppm):  $\delta = 2.35$  (s, 3H, 5- $\text{CH}_3$ ); 2.49 (s, 3H, 3- $\text{CH}_3$ ); 6.46 (s, 1H, CH); 7.38–7.41 (d, 2H, Ph,  $J = 8.83$  Hz); 7.71–7.74 (d, 2H, Ph,  $J = 8.83$  Hz).  $^{13}\text{C}$  NMR (75 MHz,  $\text{CDCl}_3$ , ppm):  $\delta = 10.98$ ; 11.74; 109.14; 126.14; 127.66; 131.45; 133.65; 147.00; 147.88.  $^{19}\text{F}$  NMR (282 MHz,  $\text{CDCl}_3$ , ppm):  $\delta = -149.40$ ;  $-149.44$ . Analysis: calcd for  $\text{C}_{11}\text{H}_{12}\text{BBrF}_4\text{N}_2$ : C 38.98 H 3.57 N 8.27. Found: C 38.78 H 3.61 N 8.22.

1-(p-methylphenyl)-3,5-dimethylpyrazolium tetrafluoroborate (3d): Yield: 90% (off-white solid); m.p: 140 °C; IR (ATR,  $\text{cm}^{-1}$ )  $\nu_{\text{max}} = 3236$ ; 3045; 2926–2885; 1639; 1578; 1517; 1432; 1065; 1036; 827.  $^1\text{H}$  NMR (300 MHz,  $\text{CDCl}_3$ , ppm):  $\delta = 2.37$  (s, 3H, 5- $\text{CH}_3$ ); 2.47 (s, 3H, 3- $\text{CH}_3$ ); 2.58 (s, 3H, p-( $\text{CH}_3$ )-Ph); 6.41 (s, 1H, CH); 7.35–7.38 (d, 2H, Ph,  $J = 8.60$  Hz); 7.4–7.43 (d, 2H, Ph,  $J = 8.60$  Hz).  $^{13}\text{C}$  NMR (75 MHz,  $\text{CDCl}_3$ , ppm):  $\delta = 10.92$ ; 11.73; 21.28; 108.95; 125.65; 129.97; 130.93; 142.31; 146.91; 147.17.  $^{19}\text{F}$  NMR (282 MHz,  $\text{CDCl}_3$ , ppm):  $\delta = -149.55$ ;  $-149.61$ . Analysis: calcd for  $\text{C}_{12}\text{H}_{15}\text{BF}_4\text{N}_2$ : C 52.59 H 5.52 N 10.22. Found: C 52.25 H 5.55 N 10.16.

3,5-dimethyl-1-(p-methoxyphenyl)pyrazolium tetrafluoroborate (3e): Yield: 99.5% (milky brown solid); m.p: 104 °C; IR (ATR,  $\text{cm}^{-1}$ )  $\nu_{\text{max}} = 3382$ ; 3067; 2940–2846; 1601; 1577; 1517; 1442; 1257; 1081; 1034; 840.  $^1\text{H}$  NMR (300 MHz,  $\text{CDCl}_3$ , ppm):  $\delta = 2.35$  (s, 3H, 5- $\text{CH}_3$ ); 2.56 (s, 3H, 3- $\text{CH}_3$ ); 3.89 (s, 3H, p-( $\text{OCH}_3$ )-Ph); 6.39 (s, 1H, CH); 7.06–7.09 (d, 2H, Ph,  $J = 9.05$  Hz); 7.39–7.42 (d, 2H, Ph,  $J = 9.05$  Hz).  $^{13}\text{C}$  NMR (75 MHz,  $\text{CDCl}_3$ , ppm):  $\delta = 10.87$ ; 11.60; 55.75; 108.73; 115.40; 124.95; 127.56; 146.86; 147.14; 161.72.  $^{19}\text{F}$  NMR (282 MHz,  $\text{CDCl}_3$ , ppm):  $\delta = -149.74$ ;  $-149.79$ . Analysis: calcd for  $\text{C}_{12}\text{H}_{15}\text{BF}_4\text{N}_2\text{O}$ : C 49.69 H 5.21 N 9.66. Found: C 49.38 H

5.25 N 9.6.

### 2.3. X-ray diffraction analysis

Suitable crystals of 2a and 3d were selected for data collection which was performed on a D8-QUEST diffractometer equipped with a graphite-monochromatic Mo- $K_\alpha$  radiation at 296 K. The structure was solved by direct methods using SHELXS-2013 [27] and refined by full-matrix least-squares methods on  $F^2$  using SHELXL-2013 [28]. All non-hydrogen atoms were refined with anisotropic parameters. The H atom of N atom was located in a difference map and refined freely. The other H atoms were located from different maps and then treated as riding atoms with C–H distance of 0.93–0.96 Å. The following procedures were implemented in our analysis: data collection: Bruker APEX2 [29]; program used for molecular graphics were as follow: MERCURY programs [30]; software used to prepare material for publication: WinGX [31].

## 3. Results and discussion

### 3.1. Synthesis and characterization

The synthetic route for 1-aryl-3,5-dimethylpyrazolium salts are outlined in Fig. 1. 1-aryl-3,5-dimethyl-1H-pyrazole derivatives (1a–1e) were synthesized from arylhydrazinium hydrochloride derivatives and acetylacetone under MW irradiation. The reaction of 1-aryl-3,5-dimethyl-1H-pyrazole derivatives with conc. HCl (37%) and  $\text{HBF}_4$  (48% in water) gave compounds 2a–2e and 3a–3e, respectively at room temperature.

The chemical structure of the synthesized 1-aryl-3,5-dimethylpyrazolium salts was elucidated with the FTIR,  $^1\text{H}$  NMR,  $^{13}\text{C}$  NMR,  $^{19}\text{F}$  NMR (3a–3e) and elemental analysis. The FTIR spectra of all the salts show the characteristic  $\nu(\text{C}-\text{H})$  stretching bands of the 3,5-dimethylpyrazole ring at around 3029–3117  $\text{cm}^{-1}$ . In addition,  $\nu(\text{C}=\text{N})$  and  $\nu(\text{C}=\text{C})$  stretching vibrations of the 3,5-dimethylpyrazolium ring is observed at ca. 1602–1578  $\text{cm}^{-1}$  and at ca. 1497–1429  $\text{cm}^{-1}$ , respectively. The  $^1\text{H}$  NMR and  $^{13}\text{C}$  NMR spectra of salts are also compatible with the chemical structure of all salts and verify the 3,5-dimethylpyrazole ring and the aryl ring at the N-1 nitrogen atom of the 3,5-dimethylpyrazole heterocycle.  $^{19}\text{F}$  NMR spectra of 3a–3e show two typical signals of  $[\text{BF}_4]^-$  anion at ca.  $\delta (-149.40)$ – $(-149.81)$ .

### 3.2. Thermal properties

Two of the salts namely 2e and 3b fulfill the formal definition and are ionic liquids, while rest of the synthesized salts have a melting point above 100 °C and do not meet the ionic liquid criteria. Both the electronic influence of substituent at the para position of

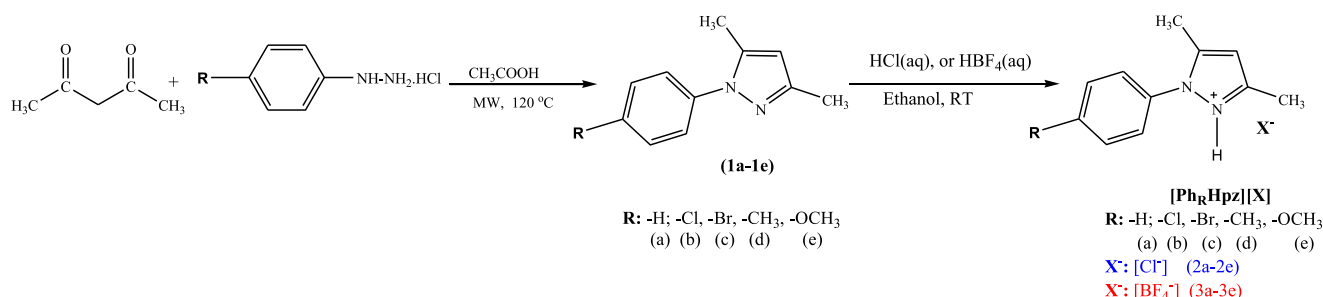


Fig. 1. Synthesis of the 1-aryl-3,5-dimethylpyrazolium salts via two step reaction.

the phenyl ring and the effect of anion on the melting point of 1-aryl-3,5-dimethylpyrazolium salts were investigated (Fig. 2). According to the results obtained, both the electron-withdrawing ( $-\text{Cl}$ ,  $-\text{Br}$ ) and the electron-donating ( $-\text{CH}_3$ ,  $-\text{OCH}_3$ ) p-substituents and the anions ( $[\text{Cl}^-]$  and  $[\text{BF}_4^-]$ ) affect the melting points of 1-aryl-3,5-dimethylpyrazolium based protic salts. The melting points of ionic salts which have 1-(p-methylphenyl)-3,5-dimethylpyrazolium cation decrease in the order of  $[\text{BF}_4^-] < [\text{Cl}^-]$  while the ionic salts which have 3,5-dimethyl-1-(p-methoxyphenyl)pyrazolium cation increase in the order of  $[\text{BF}_4^-] > [\text{Cl}^-]$ . The inductive effect of the methyl group is very different compared to the mesomeric effect of methoxy substituent, which interacts via the  $\pi$ -system. Also, melting points of the salts which contain p-Cl substituent on the phenyl ring are lower than those of the salts containing p-Br substituent for all the anions.

The melting points for the investigated 1-aryl-3,5-dimethylpyrazolium salts with  $[\text{BF}_4^-]$  anion were found lower in most cases than those for their corresponding aprotic 3,5-dimethylpyrazolium based congeners (Table 1). The melting points of aprotic pyrazolium ILs increase in the order of  $\text{Br} > \text{CH}_3 > \text{H} > \text{Cl} > \text{OCH}_3$  while the melting points of protic ILs increase in the order of  $\text{CH}_3 > \text{Br} > \text{H} > \text{OCH}_3 > \text{Cl}$ .

Thermal stability of the ionic liquids 2e and 3b was investigated using thermogravimetric analysis. As shown in Fig. 3, thermal decomposition temperatures of 2e and 3b ionic liquids were found as 151.31 °C and 215.95 °C, respectively. With regard to the anion effect, the thermal stability of  $[\text{BF}_4^-]$  containing ionic liquid is higher than  $[\text{Cl}^-]$  containing ionic liquids. In addition, electron withdrawing p-Cl substituted 3b salt has higher thermal decomposition temperature than electron donating p-OMe substituted 2e salt.

### 3.3. Crystal structures of 2a and 3d

The crystal structures of 2a and 3d salts with atom labelling are shown in Supp. Figure 1 and Supp. Figure 2, respectively. Details of data collection and crystal structure determinations are also given

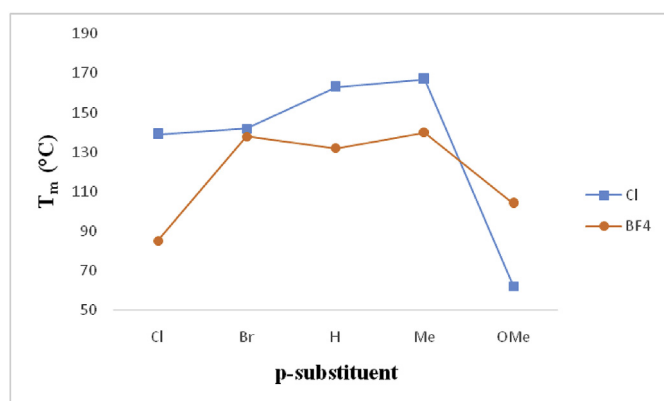


Fig. 2. Melting points of 1-aryl-3,5-dimethylpyrazolium  $[\text{Cl}^-]$  and  $[\text{BF}_4^-]$  salts.

Table 1  
Melting points (Mp) of protic and aprotic pyrazolium based ionic liquids.

Protic Pyrazolium ILs		Aprotic Pyrazolium ILs [26]	
$[\text{Ph}_R\text{HPz}][\text{BF}_4]$	Mp (°C)	$[\text{Ph}_R\text{C}_1\text{Pz}][\text{BF}_4]$ C <sub>1</sub> : methyl	Mp (°C)
R:-H	132	R:-H	145
R:-Cl	85	R:-Cl	133
R:-Br	138	R:-Br	161
R:-CH <sub>3</sub>	140	R:-CH <sub>3</sub>	148
R:-OCH <sub>3</sub>	104	R:-OCH <sub>3</sub>	76

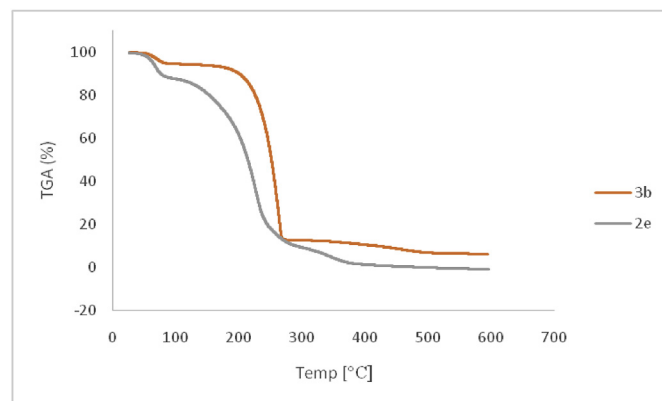


Fig. 3. TGA curves of the compounds 2e and 3b.

in Table 2. The molecules of 2a are linked into sheets by  $\text{N}-\text{H}\cdots\text{Cl}$  and  $\text{C}-\text{H}\cdots\text{Cl}$  hydrogen bonds while the molecules of 3d are linked by combination of  $\text{N}-\text{H}\cdots\text{F}$  and  $\text{C}-\text{H}\cdots\text{F}$  hydrogen bonds (Supp. Table 1). In 2a, the combination of hydrogen bonds generates edge-fused  $R_6^2(19)R_6^3(28)$  rings which is running parallel to the  $[010]$  direction (Fig. 4). In 3d, the  $\text{C}19-\text{H}20\cdots\text{F}28^{\text{II}}$  and  $\text{N}1-\text{H}30\cdots\text{F}27$  hydrogen bonds produce centrosymmetric  $R_4^4(16)$  ring centered at  $(1/2, 1/2, 1/2)$  (Fig. 5).

### 3.4. Optimized geometries

The geometries of the cations, anions and ionic salts were optimized by DFT/B3LYP and M06-2X methods and 6-311 + G (d,p) basis set. With the vibrational frequency calculations, we determined that the optimized structures are on real local minima without imaginary frequencies. All calculations were performed with Gaussian 09 software package [32]. The M06-2X functional is one of the best functional for the study of hydrogen bonding [33]. H-bonding plays a significant role for many ionic liquids to determine the secondary structuring and for practical applications [34].

Firstly, the ion geometries of five pyrazole cations with substituents  $-\text{H}$ ,  $-\text{Cl}$ ,  $-\text{Br}$ ,  $-\text{CH}_3$ ,  $-\text{OCH}_3$  and of two anions  $[\text{Cl}^-]$ , and  $[\text{BF}_4^-]$  were optimized using DFT/B3LYP and M06-2X/6-311 + G (d,p). To determine the most stable conformations for each ionic salt, their different initial geometries were optimized at the same

Table 2  
Crystal data and structure refinement parameters for 2a and 3d salts.

	2a	3d
Empirical formula	$\text{C}_{11}\text{H}_{13}\text{N}_2\text{Cl}$	$\text{C}_{12}\text{H}_{15}\text{N}_2\text{BF}_4$
Formula weight	208.68	274.07
Crystal system	Monoclinic	Monoclinic
Space group	$P2_1/n$	$P2_1/c$
a (Å)	7.6831 (13)	11.6379 (9)
b (Å)	13.504 (2)	9.2436 (7)
c (Å)	10.6848 (16)	13.8139 (9)
$\beta$ (°)	100.129 (6)	114.470 (3)
V (Å <sup>3</sup> )	1091.3 (3)	1352.57 (17)
Z	4	4
$D_c$ (g cm <sup>-3</sup> )	1.270	1.346
$\mu$ (mm <sup>-1</sup> )	0.31	0.12
$\theta$ range (°)	3.0–28.2	2.9–26.3
Measured refls	37364	29283
Independent refls	2744	2657
$R_{\text{int}}$	0.092	0.080
S	1.05	1.06
R1/wR2	0.089/0.175	0.095/0.229
$\Delta\rho_{\text{max}}/\Delta\rho_{\text{min}}$ (eÅ <sup>-3</sup> )	0.34/-0.32	0.54/-0.35

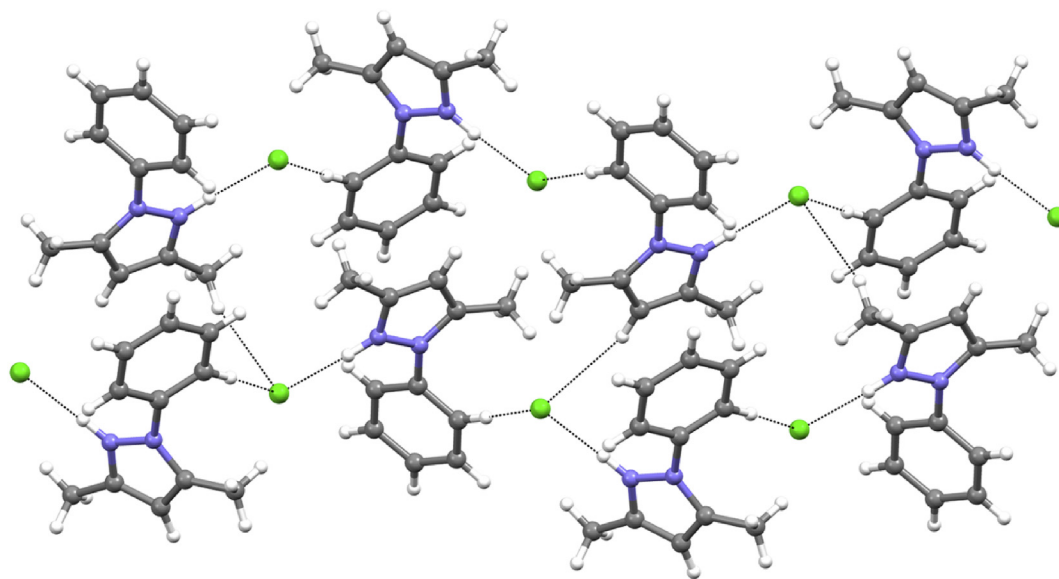


Fig. 4. Crystal structure of 2a, showing the formation of a chain along [010] generated by N-H...Cl and C-H...Cl hydrogen bonds.

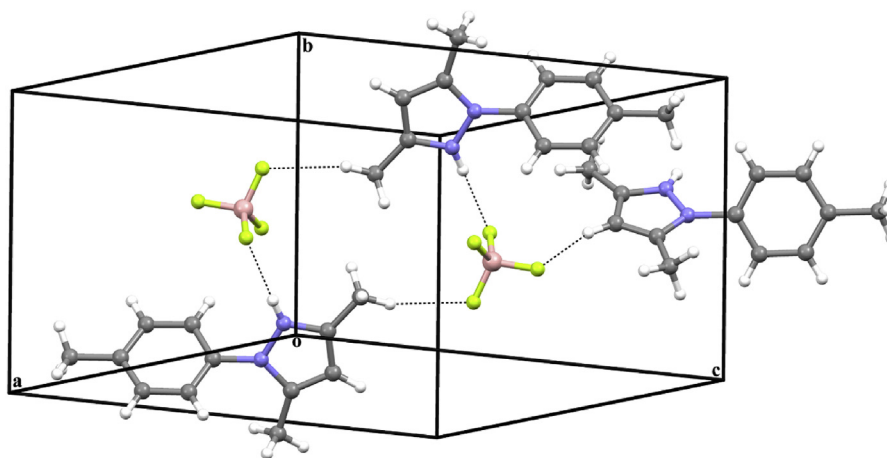


Fig. 5. Crystal structure of 3d, showing the formation of a  $R_4^1(16)$  ring generated by N-H...F and C-H...F hydrogen bonds.

level of theory. The most stable conformations of 2a and 3d (with atom numbering) and the crystal structures of 2a and 3d ionic salts are given in Fig. 6. The optimized structures of all ionic salts are given in Supp Fig 3. The selected optimized structure parameters are shown in Table 3.

As seen in Supp Figure 3, ionic salts which are composed of same anions have a similar structure for different cations. In ion pairs, heteroatoms of anions operate as proton acceptors and N–H, C–H bonds of the cation as proton donors.

For finding the most stable geometry of 2a, chlorine atom was brought near two possible positions N5–H25 and C2–H4. The most stable optimized geometry was obtained for 2a with N5–H25...Cl structure and chlorine atoms take place in the plane of the pyrazole ring as seen in Fig. 6. The other ionic salts 2b–2e have also similar structural properties with 2a (Supp Fig. 3).  $[\text{Cl}^-]$  anion catches H from the cation to form H–Cl in optimized geometries, but H is bonded to the N atom by the crystal structure of 2a as seen in Fig. 6. The distance of H–Cl is obtained in the range of 1.353 and 1.365 Å by B3LYP calculations (1.366 and 1.381 Å by M06-2X calculations). H–Cl bond length is identified by X-ray as 2.028 Å. Both of the

computed H–Cl bonds are shorter than the experimental ones. All of the experimental H–Cl bond lengths values lie between the covalent bond distance (1.31 Å) and the van der Waals distance (2.95 Å) for H–Cl [35] but are also closer to the covalent bond distance. The corresponding experimental bond length is closer to the van der Waals distance. The N–H bond distances of salts 2a–2e are larger than the covalent bond distance of N–H (1.31 Å) with the values of 1.646 Å–1.693 Å by B3LYP calculations, while the N–H bond distance by the crystal structure of 2a is shorter with the value of 0.93 Å. M06-2X method predicts these values between 1.561 Å and 1.604 Å. Accordingly, M06-2X method predicts lengths of H–Cl bonds longer than the B3LYP method, while it predicts lengths of N–H bonds shorter. However, in general, B3LYP and M06-2X calculations give similar optimized geometry shapes (Table 3).

In the most stable geometries of 3a–3e salts,  $[\text{BF}_4^-]$  anion is favourable to move near the N5–H25 fragment. The distances of F27...H30 are in the range of 1.510 Å– 1.642 Å (1.495 Å–1.505 Å with the M062X method), while the distances of F29...H14 and F26...H20 are between 2.134 Å and 3.082 Å (2.273 Å–2.373 Å with the M06-2X method) [36]. The hydrogen bonding angles of

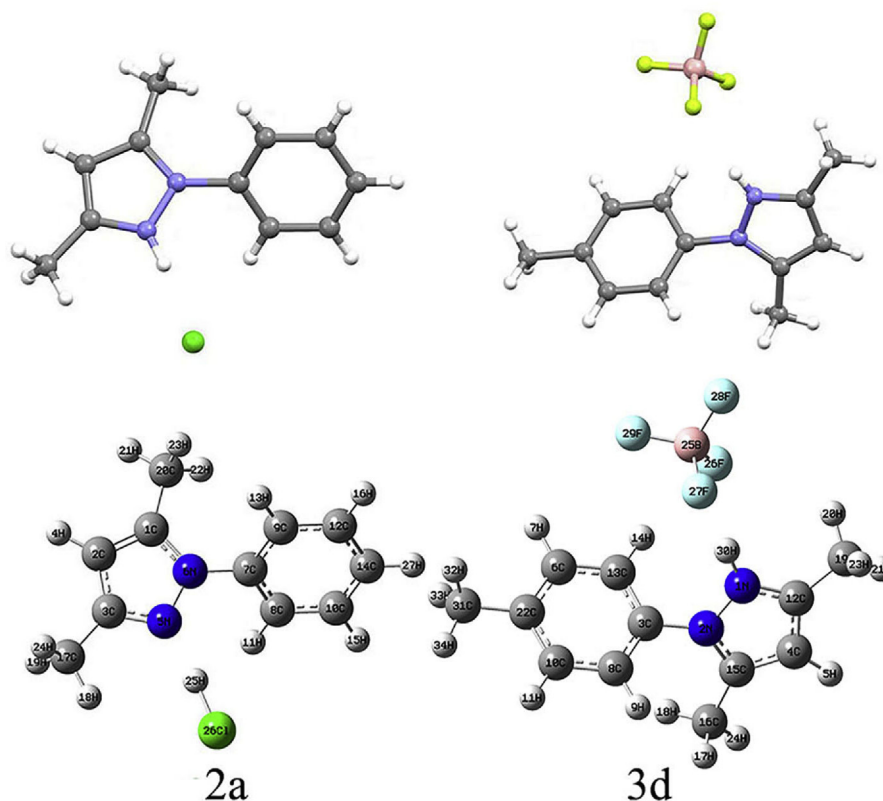


Fig. 6. The crystal structures (upper) and the optimized geometries (bottom) of  $[\text{Ph}_R\text{HPz}][\text{Cl}]$  (R: -H), and  $[\text{Ph}_R\text{HPz}][\text{BF}_4]$  (R:  $-\text{CH}_3$ ).

Table 3

Selected Bond Lengths (Å), Bond Distances (Å), Bond Angles ( $^\circ$ ) and Dihedral Angles ( $^\circ$ ) of ionic salts.

	Cl26–H25	N5–H25	N5–H25...Cl26	N5–N6–C7–C9	Cl26...H25–N5–C3		
2a	1.357	1.678	175.7	–131.1	11.1		
2b	1.353	1.693	176.4	–131.4	14.4		
2c	1.353	1.692	176.9	–129.7	13.6		
2d	1.360	1.665	175.9	–128.4	8.6		
2e	1.365	1.646	175.9	–124.3	8.6		
	F1–H25	F2–H15	F3–H18	N5–H25	N5–H25...F1	N5–H25...F2	N5–N6–C7–C9
3a	1.517	2.179	2.231	1.060	173.8	114.3	122.5
3b	1.514	2.134	2.242	1.061	173.6	113.4	122.8
3c	1.514	2.143	2.227	1.061	173.5	113.5	120.9
3d	1.523	2.186	2.225	1.059	173.0	114.4	122.0
3e	1.532	2.169	2.240	1.058	173.0	114.0	120.6

$\text{N1–H30}\cdots\text{F27}$  for 3a–3e are predicted to be  $168.0^\circ$ – $173.8^\circ$  by B3LYP calculations and  $173.1^\circ$ – $174.4^\circ$  by M06-2X calculations. The corresponding value for 3d is obtained as  $161.2^\circ$  by crystal structure.

The phenyl ring is twisted with pyrazole ring in all ionic salts. In the most stable geometries of 3a–3e, the dihedral angle  $\text{N1–N2–C3–C8}$  is kept between  $109.7^\circ$ – $122.8^\circ$  by B3LYP calculations and  $128.3$ – $131.8^\circ$  by M06-2X calculations, while 2a–2e have this dihedral angle in the range of  $-124.3^\circ$  and  $-131.4^\circ$  ( $-131.7^\circ$ – $-137.0^\circ$  by M06-2X calculations). The corresponding value for the crystal structure of 2a is  $-130.3^\circ$ .

### 3.5. Molecular electrostatic potential (MEP) analysis

The molecular electrostatic potential maps show the charge distribution of molecules three-dimensionally. The MEPs of the anions ( $[\text{Cl}^-]$  and  $[\text{BF}_4^-]$ ) and the cations of 1-aryl-3,5-

dimethylpyrazoles and the MEPs of the 1-aryl-3,5-dimethylpyrazolium based ionic liquids/salts assessed at B3LYP/6-311 + G (d,p) level of theory are given in Fig. 7 and Fig. 8, respectively.

The maps of the molecular electrostatic potential surface for the ground state geometry of the ionic salts give an idea about the nucleophilic (red in colour) or electrophilic regions (blue in colour) of the molecules (Supp Figure 3). The red colour on all the surface of the anions indicates that they are nucleophilic, while blue colour on the cations surface represents their electrophilic character (Fig. 7). As seen in Fig. 8, the negative potential sites in  $[\text{Cl}^-]$ , and  $[\text{BF}_4^-]$  anions distribute on chlorine and fluorine atoms and the positive potential sites in 3,5-dimethyl-1-phenylpyrazolium cation distribute on the methyl group of the 3,5-dimethylpyrazole ring. The map of the MEP of all ionic salts generally illustrates a similar pattern with 2a and 3a salts (Supp Figure 3).

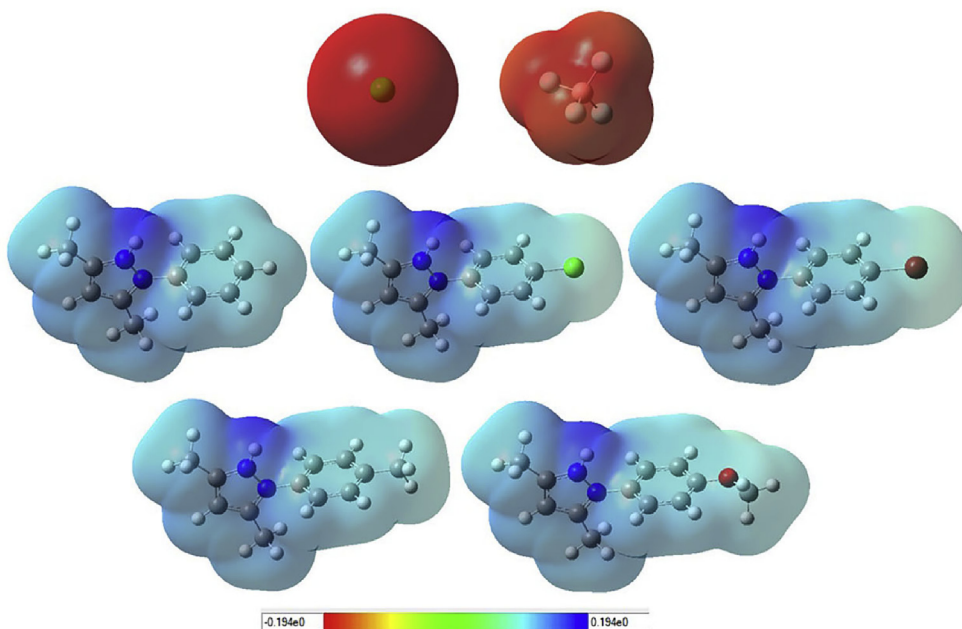


Fig. 7. Calculated electrostatic potential surfaces on the molecular surface of the anions ( $[\text{Cl}^-]$  and  $[\text{BF}_4^-]$ ) and the cations of 1-aryl-3,5-dimethylpyrazoles.

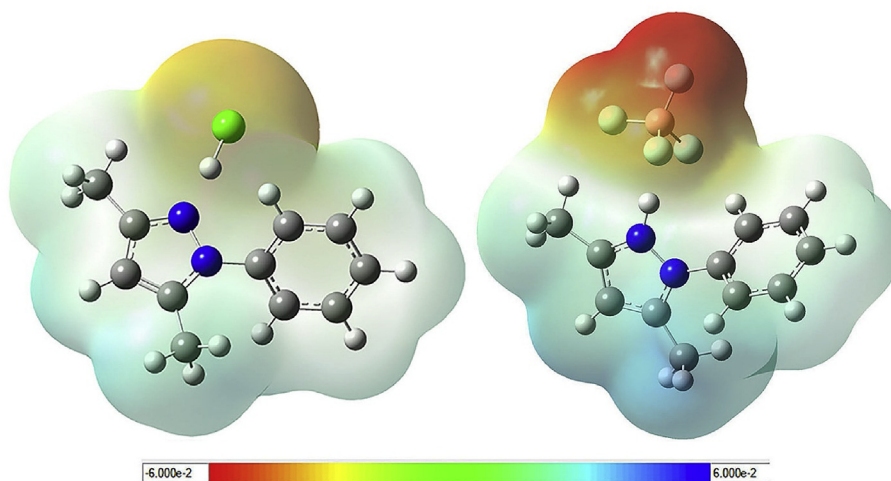


Fig. 8. Maps of the molecular electrostatic potential surface of  $[\text{Ph}_R\text{HPz}][\text{Cl}]$ , and  $[\text{Ph}_R\text{HPz}][\text{BF}_4]$  (R:H).

### 3.6. Electrochemical window (EW)

The electrochemical window of the 1-aryl-3,5-dimethylpyrazolium based ionic liquids/salts which have  $[\text{Cl}^-]$  and  $[\text{BF}_4^-]$  anions was measured with cyclic voltammetry (CV) at 25 °C by using glassy carbon macro electrode (surface area:  $7.065 \times 10^{-2} \text{ cm}^2$ ) as a working electrode, Pt as a counter electrode and Ag/AgCl as a reference electrode. The experimentally determined EW values of ionic salts are between 2.77 and 2.98 (Table 4). The experimental EW values of 3a-3e salts are generally lower than their 1-aryl-2,3,5-trimethylpyrazolium  $[\text{BF}_4^-]$  analogs [26].

The highest occupied molecular orbital (HOMO) and the lowest unoccupied molecular orbital (LUMO) energy levels, the potentials of cathodic ( $V_{\text{Cl}}$ ) and anodic limits ( $V_{\text{AL}}$ ) of the salts were calculated by DFT/B3LYP and M06-2X/6-311 + G (d,p) in gas phase and the results were given in Table 5.

The correlation coefficients between the calculated LUMO

energies of  $[\text{Ph}_R\text{HPz}][\text{BF}_4^-]$  ionic salts (3a-3e) and those of their corresponding cations in the gas phase were obtained as 0.9921 (by B3LYP calculations) and 0.9648 (by M06-2X calculations) (Supp. Figure 4). These results clearly indicate that LUMO energy levels are well correlated. Accordingly, it can be presumed that the LUMO energy levels of the cations determine the resistance of these salts against reduction.

The cathodic stability of the salts against reduction is ordered as R:  $\text{OCH}_3 > \text{CH}_3 > \text{H} > \text{Br} > \text{Cl}$  both for B3LYP and M06-2X methods in gas phase. According to the results obtained, electron donating substituents ( $-\text{CH}_3$ ,  $-\text{OCH}_3$ ) at the para position of the phenyl ring generally increase EW of the salts (stabilize the cation) while electron-withdrawing substituents ( $-\text{Cl}$ ,  $-\text{Br}$ ) decrease EW of the salts (destabilize the cation). These results are consistent with the results obtained for 1-aryl-2,3,5-trimethylpyrazolium cations ( $[\text{Ph}_R\text{C}_1\text{pz}]^+$ , R: 4-Cl, 4-Br, 4-Me, 4-OMe, 4-NO<sub>2</sub>; C<sub>1</sub>: methyl) and para-X-phenyl methylimidazolium ( $[\text{X-PhMIM}]^+$ : X = OCH<sub>3</sub>, CH<sub>3</sub>,

**Table 4**Cathodic and anodic potentials vs. Ag/Ag<sup>+</sup> for EWs of the protic pyrazolium ionic liquids/salts using GC macro-electrode as a working electrode at 25 °C.

Entry	Salts	E <sub>cathodic</sub> (V)	E <sub>anodic</sub> (V)	EW(V)	Entry	Salts	E <sub>cathodic</sub> (V)	E <sub>anodic</sub> (V)	EW(V)
1	2a	-2.00	0.79	<b>2.79</b>	6	3a	-1.13	1.65	<b>2.78</b>
2	2b	-2.04	0.74	<b>2.78</b>	7	3b	-1.43	1.36	<b>2.79</b>
3	2c	-2.01	0.76	<b>2.77</b>	8	3c	-1.42	1.36	<b>2.78</b>
4	2d	-2.25	0.70	<b>2.95</b>	9	3d	-1.49	1.38	<b>2.85</b>
5	2e	-2.29	0.69	<b>2.98</b>	10	3e	-1.62	1.22	<b>2.84</b>

**Table 5**E<sub>LUMO</sub> and E<sub>HOMO</sub> (eV) of [Ph<sub>R</sub>Hpz][BF<sub>4</sub>] salts, E<sub>LUMO</sub>, E<sub>HOMO</sub> (eV), potentials of cathodic (V<sub>CL</sub>) and anodic (V<sub>AL</sub>) limits of individual ions and electrochemical window (EW) of all salts calculated by density functional theory (DFT) at M06-2X and B3LYP methods using 6-311 + G (d,p) basis set in gas phase.

[Ph <sub>R</sub> Hpz][BF <sub>4</sub> ]	B3LYP					M06-2X				
	R = H	Cl	Br	CH <sub>3</sub>	OCH <sub>3</sub>	H	Cl	Br	CH <sub>3</sub>	OCH <sub>3</sub>
E <sub>LUMO</sub>	-1.97847	-2.14807	-2.14017	-1.87650	-1.76058	-0.95240	-1.12220	-1.13288	-0.80634	-0.68110
E <sub>HOMO</sub>	-7.70028	-7.83280	-7.46817	-7.42844	-6.95115	-8.93186	-8.81540	-8.69431	-8.64452	-8.19607
<b>[Ph<sub>R</sub>Hpz]<sup>+</sup></b>										
E <sub>LUMO</sub>	-5.16255	-5.26132	-5.24826	-5.07057	-5.01043	-4.00062	-4.09913	-4.07681	-3.89341	-3.87436
E <sub>HOMO</sub>	-10.87640	-10.51775	-10.22005	-10.53217	-9.78114	-12.27288	-11.87505	-11.53954	-11.88104	-11.16266
V <sub>CL</sub> /V	5.16255	5.26132	5.24826	5.07057	5.01043	4.00062	4.09913	4.07681	3.89341	3.87436
V <sub>AL</sub> /V	10.87640	10.51775	10.22005	10.53217	9.78114	12.27288	11.87505	11.53954	11.88104	11.16266
<b>Anions</b>										
	[Cl <sup>-</sup> ]	[BF <sub>4</sub> ]				[Cl <sup>-</sup> ]	[BF <sub>4</sub> ]			
E <sub>LUMO</sub>	5.89344	4.39437				6.80448	5.74922			
E <sub>HOMO</sub>	-7.68722	-4.52553				-2.18916	-3.08795			
V <sub>CL</sub> /V	-5.89344	-4.39437				-6.80448	-5.74922			
V <sub>AL</sub> /V	7.68722	4.52553				2.18916	3.08795			
<b>EWcalc/V</b>										
[Ph <sub>R</sub> Hpz][Cl]	2.52467	2.42590	2.43896	2.61665	2.67679	-1.81146	-1.90997	-1.88765	-1.70425	-1.68520
[Ph <sub>R</sub> Hpz][BF <sub>4</sub> ]	-0.63702	-0.73579	-0.72273	-0.54504	-0.48490	-0.91267	-1.01118	-0.98886	-0.80546	-0.78641

and NO<sub>2</sub>) cations [26,37].

The electrochemical windows of all the salts were calculated theoretically by using the following expression, for comparison with the experimentally determined EW values, and the results are given in Table 5;

$$EW = V_{AL} - V_{CL} = \frac{-\epsilon_{HOMO}}{e} - \frac{-\epsilon_{LUMO}}{e} = \frac{\epsilon_{LUMO} - \epsilon_{HOMO}}{e}$$

Theoretically calculated EW values of the [BF<sub>4</sub>]<sup>-</sup> and [Cl<sup>-</sup>] salts follow the same order as R: OMe > Me > H > Br > Cl both for B3LYP and M06-2X methods. However, for the [BF<sub>4</sub>]<sup>-</sup> and [Cl<sup>-</sup>] salts the experimentally determined EW values in solvent acetonitrile are ordered as R: Me > OMe > Cl > H = Br, R: OMe > Me > H > Cl > Br, respectively. The correlation between the theoretical and the experimental EW values of the [Cl<sup>-</sup>] salts are reasonably good with correlation coefficients of 0.9027 (by M06-2X calculations) and 0.9024 (by B3LYP calculations). The correlation between the theoretical and the experimental EW values of the [BF<sub>4</sub>]<sup>-</sup> salts is moderate with a value of 0.7838 (by M06-2X calculations) and 0.7419 (by B3LYP calculations) (Fig. 9).

#### 4. Conclusions

In conclusion, a series of new 1-aryl-3,5-dimethylpyrazolium based protic ionic liquids/salts ([Ph<sub>R</sub>Hpz][X], R: -H, -Cl, -Br, -CH<sub>3</sub>, -OCH<sub>3</sub>, X: chloride [Cl<sup>-</sup>] and tetrafluoroborate [BF<sub>4</sub>]<sup>-</sup>) were synthesized and characterized. Melting points of all the salts and thermal stabilities of two ionic liquids (2e and 3b) were determined. According to the results obtained, both the electron-withdrawing (-Cl, -Br) and the electron-donating (-CH<sub>3</sub>, -OCH<sub>3</sub>) p-substituents and type of the anions ([Cl<sup>-</sup>], [BF<sub>4</sub>]<sup>-</sup>) affect the melting points of 1-aryl-3,5-dimethylpyrazolium protic salts.

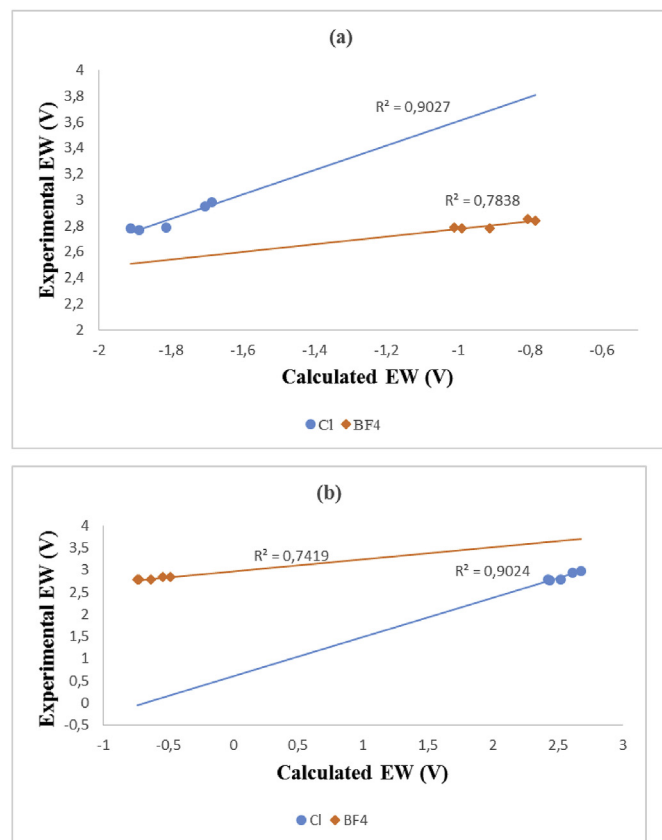


**Fig. 9.** The correlation between calculated and experimental EW values of the ionic salts (a) by M06-2X calculations (b) by B3LYP calculations.

Electrochemical windows of all the salts were calculated theoretically and compared with the experimentally determined EW values. A reasonably good correlation was found between the theoretical and experimental EW values of the salts. Electrostatic surface potentials for the ground state geometry of the ionic salts were calculated to gain insight into the electron density distribution. The electrostatic potential maps indicate that the negative charge is located on the anion and the positive charge on the cation.

### Acknowledgements

The authors are grateful to the Research Foundation of Gazi University (Project no. 05/2012-21) for supporting this study. The authors acknowledge Scientific and Technological Research Application and Research Centre, Sinop University, Turkey, for the use of the Bruker D8 QUEST diffractometer.

### Supplementary data

This material includes  $^1\text{H}$  NMR,  $^{13}\text{C}$  NMR, and  $^{19}\text{F}$  NMR (3a–3e) spectra; and Cyclic Voltammograms of all the pyrazolium salts. Crystallographic data for the structural analysis have been deposited with the Cambridge Crystallographic Data Centre, CCDC No. 1873253 for 2a and 1877556 for 3d. Copies of this information may be obtained free of charge from the Director, CCDC, 12 Union Road, Cambridge CB2 1EZ, UK (fax: +44-1223-336033; e-mail: [deposit@ccdc.cam.ac.uk](mailto:deposit@ccdc.cam.ac.uk) or [www: http://www.ccdc.cam.ac.uk](http://www.ccdc.cam.ac.uk)).

### Appendix A. Supplementary data

Supplementary data related to this article can be found at <https://doi.org/10.1016/j.molstruc.2018.12.027>.

### References

- [1] T.L. Greaves, C.J. Drummond, Protic ionic liquids: properties and applications, *Chem. Rev.* 108 (2008) 206–237.
- [2] A. Mirjafari, L.N. Pham, J.R. McCabe, N. Mobarrez, E.A. Salter, A. Wierzbicki, K.N. West, R.E. Sykora, J.H. Davis Jr., Building a bridge between aprotic and protic ionic liquids, *RSC Adv* 3 (2013) 337–340.
- [3] M.V.S. Oliveira, B.T. Vidal, C.M. Melo, R.C.M. de Miranda, C.M.F. Soares, J.A.P. Coutinho, S.P.M. Ventura, S. Mattedi, A.S. Lima, (Eco)toxicity and biodegradability of protic ionic liquids, *Chemosphere* 147 (2016) 460–466.
- [4] C.A. Angell, Y. Ansari, Z. Zhao, Ionic liquids: past, present and future, *Faraday Discuss* 154 (2012) 9–27.
- [5] T.L. Greaves, K. Ha, B.W. Muir, S.C. Howard, A. Weerawardena, N. Kirby, C.J. Drummond, Protic ionic liquids (PILs) nanostructure and physicochemical properties: development of high-throughput methodology for PIL creation and property screens, *Phys. Chem. Chem. Phys.* 17 (2015) 2357–2365.
- [6] T.L. Greaves, C.J. Drummond, Protic ionic liquids: evolving structure–property relationships and expanding applications, *Chem. Rev.* 115 (2015) 11379–11448.
- [7] R. Hayes, S. Imberti, G.G. Warr, R. Atkin, The nature of hydrogen bonding in protic ionic liquids, *Angew. Chem. Int. Ed.* 52 (2013) 4623–4627.
- [8] K. Fumino, E. Reichert, K. Wittler, R. Hempelmann, R. Ludwig, Low-frequency vibrational modes of protic molten salts and ionic liquids: detecting and quantifying hydrogen bonds, *Angew. Chem. Int. Ed.* 51 (2012) 6236–6240.
- [9] J. Reichenbach, S.A. Ruddell, M. Gonzalez-Jimenez, J. Lemes, D.A. Turton, D.J. France, K. Wynne, Phonon-like hydrogen-bond modes in protic ionic liquids, *J. Am. Chem. Soc.* 139 (2017) 7160–7163.
- [10] X. Lu, G. Burrell, F. Separovic, C. Zhao, Electrochemistry of room temperature protic ionic liquids: a critical assessment for use as electrolytes in electrochemical applications, *J. Phys. Chem. B* 116 (2012) 9160–9170.
- [11] S. Menne, T. Vogl, A. Balducci, The synthesis and electrochemical characterization of bis(fluorosulfonyl)imide-based protic ionic liquids, *Chem. Commun.* 51 (2015) 3656–3659.
- [12] C. Brigouleix, M. Anouti, J. Jacquemin, M. Caillon-Caravanier, H. Galiano, D. Lemordant, Physicochemical characterization of morpholinium cation based protic ionic liquids used as electrolytes, *J. Phys. Chem. B* 114 (2010) 1757–1766.
- [13] J.P. Hallett, T. Welton, Room-temperature ionic liquids: solvents for synthesis and catalysis 2, *Chem. Rev.* 111 (2011) 3508–3576.
- [14] C.G. Adam, G.G. Fortunato, P.M. Mancini, Nucleophilic and acid catalyst behavior of a protic ionic liquid in a molecular reaction media. Part 1, *J. Phys. Org. Chem.* 22 (2009) 460–465.
- [15] S. Sunitha, S. Kanjilal, P.S. Reddy, R.B.N. Prasad, An efficient and chemoselective bronsted acidic ionic liquid-catalyzed N-Boc protection of amines, *Tetrahedron Lett* 49 (2008) 2527–2532.
- [16] M. Dabiri, P. Salehi, M. Bahramnejad, M. Baghbanzadeh, Ecofriendly and efficient procedure for hetero-Michael Addition reactions with an acidic ionic liquid as catalyst and reaction medium, *Monatsh. Chem.* 143 (2012) 109–112.
- [17] C. Mukhopadhyay, A. Datta, P.K. Tapaswi, Halogen-free room-temperature bronsted acidic ionic liquid [Hmim]<sup>+</sup> HSO<sub>4</sub><sup>-</sup> as a recyclable green “dual reagent” catalysis for the synthesis of triarylmethanes (Trams), *Synth. Commun.* 42 (2012) 2453–2463.
- [18] L.C. Henderson, M.T. Thornton, N. Byrne, B.L. Fox, K.D. Waugh, J.S. Squire, L. Servinis, J.P. Delaney, H.L. Brozinski, L.M. Andrighetto, J.M. Altimari, Protic ionic liquids as recyclable solvents for the acid catalysed synthesis of diphenylmethylthioethers, *C. R. Chim.* 16 (2013) 634–639.
- [19] L. Liu, Y. Cheng, F.R. Sun, J.P. Yang, Y. Wu, Enhanced direct electron transfer of glucose oxidase based on a protic ionic liquid modified electrode and its biosensing application, *J. Solid State Electrochem.* 16 (2012) 1003–1009.
- [20] S. Ahrens, A. Peritz, T. Strassner, Tunable aryl alkyl ionic liquids (TAALs): the next generation of ionic liquids, *Angew. Chem. Int. Ed.* 48 (2009) 7908–7910.
- [21] D. Meyer, T. Strassner, 1,2,4-Triazole-based tunable aryl/alkyl ionic liquids, *J. Org. Chem.* 76 (2011) 305–308.
- [22] M. Lombardo, F. Pasi, C. Trombini, K.R. Seddon, W.R. Pitner, Task-specific ionic liquids as reaction media for the cobalt-catalysed cyclotrimerisation reaction of aryliethynes, *Green Chem* 9 (2007) 321–322.
- [23] T. Schulz, S. Ahrens, D. Meyer, C. Allolio, A. Peritz, T. Strassner, Electronic effects of para-substitution on the melting points of TAALs, *Chem. Asian J.* 6 (2011) 863–867.
- [24] C. Yao, W.R. Pitner, J.L. Anderson, Ionic liquids containing the tris(pentafluoroethyl)trifluorophosphate anion: a new class of highly selective and ultra hydrophobic solvents for the extraction of polycyclic aromatic hydrocarbons using single drop microextraction, *Anal. Chem.* 81 (2009) 5054–5063.
- [25] M.C. Özdemir, B. Özgün, Phenyl/alkyl-substituted-3,5-dimethylpyrazolium ionic liquids, *J. Mol. Liq.* 200 (2014) 129–135.
- [26] M.C. Özdemir, B. Özgün, Tunable aryl alkyl ionic liquids (TAALs) based on 1-aryl-3,5-dimethyl-1H-pyrazoles, *J. Mol. Liq.* 248 (2017) 314–321.
- [27] G.M. Sheldrick, A short history of SHELX, *Acta Crystallogr. A* 64 (2008) 112–122.
- [28] G.M. Sheldrick, Crystal structure refinement with SHELXL, *Acta Crystallogr. C* 71 (2015) 3–8.
- [29] APEX2, Bruker, AXS Inc. Madison, Wisconsin, USA, 2013.
- [30] C.F. Macrae, I.J. Bruno, J.A. Chisholm, P.R. Edgington, P. McCabe, E. Pidcock, L. Rodriguez-Monge, R. Taylor, J. van de Streek, P.A. Wood, Mercury CSD 2.0-new features for the visualization and investigation of crystal structures, *J. Appl. Crystallogr.* 41 (2008) 466–470.
- [31] L.J. Farrugia, WinGX and ORTEP for windows: an update, *J. Appl. Crystallogr.* 45 (2012) 849–854.
- [32] M.J. Frisch, G.W. Trucks, H.B. Schlegel, G.E. Scuseria, M.A. Robb, J.R. Cheeseman, G. Scalmani, V. Barone, B. Mennucci, G.A. Petersson, H. Nakatsuji, M. Caricato, X. Li, H.P. Hratchian, A.F. Izmaylov, J. Bloino, G. Zheng, J.L. Sonnenberg, M. Hada, M. Ehara, K. Toyota, R. Fukuda, J. Hasegawa, M. Ishida, T. Nakajima, Y. Honda, O. Kitao, H. Nakai, T. Vreven, J.A. Montgomery Jr., J.E. Peralta, F. Ogliaro, M. Bearpark, J.J. Heyd, E. Brothers, K.N. Kudin, V.N. Staroverov, T. Keith, R. Kobayashi, J. Normand, K. Raghavachari, A. Rendell, J.C. Burant, S.S. Iyengar, J. Tomasi, M. Cossi, N. Rega, J.M. Millam, M. Klene, J.E. Knox, J.B. Cross, V. Bakken, C. Adamo, J. Jaramillo, R. Gomperts, R.E. Stratmann, O. Yazyev, A.J. Austin, R. Cammi, C. Pomelli, J.W. Ochterski, R.L. Martin, K. Morokuma, V.G. Zakrzewski, G.A. Voth, P. Salvador, J.J. Dannenberg, S. Dapprich, A.D. Daniels, O. Farkas, J.B. Foresman, J.V. Ortiz, J. Cioslowski, D.J. Fox, Gaussian 09, Revision C.01, Gaussian, Inc., Wallingford CT, 2010.
- [33] P.A. Hunt, Quantum chemical modeling of hydrogen bonding in ionic liquids, *Top. Curr. Chem.* 375 (3) (2017) 59.
- [34] Y. Zhao, D.G. Truhlar, The M06 suite of density functionals for main group thermochemistry, thermochemical kinetics, noncovalent interactions, excited states, and transition elements: two new functionals and systematic testing of four M06-class functionals and 12 other functionals, *Theor. Chem. Acc.* 120 (2008) 215–241.
- [35] A. Bondi, van der Waals volumes and radii, *J. Phys. Chem.* 68 (1964) 441–451.
- [36] K. Dong, S. Zhang, D. Wang, X. Yao, Hydrogen bonds in imidazolium ionic liquids, *J. Phys. Chem. A* 110 (2006) 9775–9782.
- [37] H. Roohi, H. Houkhani, F. Rouhani, Tuning the structural, electronic and electrochemical properties of the 4-methyl-1-phenyl triazolium based [PhMeTAZ][Y1–8] ionic liquids through changing anions: a quantum chemical study, *J. Mol. Liq.* 240 (2017) 138–151.